



Cellular circadian period length inversely correlates with HbA_{1c} levels in individuals with type 2 diabetes

Flore Sinturel^{1,2,3,4} · Anne-Marie Makhoulouf^{1,2,3,4} · Patrick Meyer¹ · Christel Tran^{1,5} · Zoltan Pataky⁶ · Alain Golay⁶ · Guillaume Rey^{3,4,7} · Cédric Howald^{4,7} · Emmanouil T. Dermitzakis^{3,4,7} · Claude Pichard¹ · Jacques Philippe^{1,3} · Steven A. Brown⁸ · Charna Dibner^{1,2,3,4}

Received: 28 January 2019 / Accepted: 17 April 2019 / Published online: 27 May 2019

© Springer-Verlag GmbH Germany, part of Springer Nature 2019

Abstract

Aims/hypothesis The circadian system plays an essential role in regulating the timing of human metabolism. Indeed, circadian misalignment is strongly associated with high rates of metabolic disorders. The properties of the circadian oscillator can be measured in cells cultured in vitro and these cellular rhythms are highly informative of the physiological circadian rhythm in vivo. We aimed to discover whether molecular properties of the circadian oscillator are altered as a result of type 2 diabetes.

Methods We assessed molecular clock properties in dermal fibroblasts established from skin biopsies taken from nine obese and eight non-obese individuals with type 2 diabetes and 11 non-diabetic control individuals. Following in vitro synchronisation, primary fibroblast cultures were subjected to continuous assessment of circadian bioluminescence profiles based on lentiviral luciferase reporters.

Results We observed a significant inverse correlation ($\rho = -0.592$; $p < 0.05$) between HbA_{1c} values and circadian period length within cells from the type 2 diabetes group. RNA sequencing analysis conducted on samples from this group revealed that *ICAMI*, encoding the endothelial adhesion protein, was differentially expressed in fibroblasts from individuals with poorly controlled vs well-controlled type 2 diabetes and its levels correlated with cellular period length. Consistent with this circadian link, the *ICAMI* gene also displayed rhythmic binding of the circadian locomotor output cycles kaput (CLOCK) protein that correlated with gene expression.

Conclusions/interpretation We provide for the first time a potential molecular link between glycaemic control in individuals with type 2 diabetes and circadian clock machinery. This paves the way for further mechanistic understanding of circadian oscillator changes upon type 2 diabetes development in humans.

Data availability RNA sequencing data and clinical phenotypic data have been deposited at the European Genome-phenome Archive (EGA), which is hosted by the European Bioinformatics Institute (EBI) and the Centre for Genomic Regulation (CRG), ega-box-1210, under accession no. EGAS00001003622.

Flore Sinturel and Anne-Marie Makhoulouf contributed equally to this study.

Electronic supplementary material The online version of this article (<https://doi.org/10.1007/s00125-019-4907-0>) contains peer-reviewed but unedited supplementary material, which is available to authorised users.

✉ Charna Dibner
Charna.Dibner@hcuge.ch

¹ Department of Medicine, Division of Endocrinology, Diabetes, Hypertension and Nutrition, Faculty of Medicine, University of Geneva, Rue Michel-Servet, 1, CH-1211, 14 Geneva, Switzerland

² Department of Cell Physiology and Metabolism, Faculty of Medicine, University of Geneva, Geneva, Switzerland

³ Diabetes Center, Faculty of Medicine, University of Geneva, Geneva, Switzerland

⁴ Institute of Genetics and Genomics of Geneva (iGE3), University of Geneva, Geneva, Switzerland

⁵ Center for Molecular Diseases, Division of Genetic Medicine, Lausanne University Hospital, Lausanne, Switzerland

⁶ Division for Therapeutic Patient Education for Chronic Diseases, University Hospital of Geneva, Geneva, Switzerland

⁷ Department of Genetic Medicine and Development, Faculty of Medicine, University of Geneva, Geneva, Switzerland

⁸ Institute of Pharmacology and Toxicology, University of Zurich, Zurich, Switzerland

Research in context

What is already known about this subject?

- Metabolic disorders, including obesity and type 2 diabetes, in humans have been associated with circadian misalignment
- Properties of the human circadian oscillator in vivo correlate with those measured in primary cells cultured in vitro

What is the key question?

- Are the molecular properties of the circadian oscillator altered as a result of type 2 diabetes in humans?

What are the new findings?

- An inverse correlation was observed between HbA_{1c} values in blood and circadian period length in primary fibroblasts from individuals with type 2 diabetes
- RNA sequencing revealed that *ICAM1* expression correlated with circadian period length in primary fibroblast cells from individuals with type 2 diabetes
- *ICAM1* expression correlated with rhythmic circadian locomotor output cycles kaput (CLOCK) protein binding

How might this impact on clinical practice in the foreseeable future?

- Since alterations of circadian clock properties are concomitant with the progression of type 2 diabetes, the circadian clock might be considered as a novel therapeutic target
- Moreover, possible circadian effects of medications currently used for the treatment of metabolic diseases (e.g. metformin, which potentially alters circadian phase in rodents) should not be neglected

Keywords Circadian bioluminescence recording · Circadian clock · HbA_{1c} · Humans · *ICAM1* · Type 2 diabetes

Abbreviations

ChIP	Chromatin immunoprecipitation
CLOCK	Circadian locomotor output cycles kaput
CT	Circadian time
MCTQ	Munich Chronotype Questionnaire
O-GlcNAc	O-linked β - <i>N</i> -acetylglucosamine
qRT-PCR	Quantitative real-time PCR
RNAseq	RNA sequencing
SCN	Suprachiasmatic nuclei

Introduction

Circadian control of physiology and behaviour is driven by a master pacemaker located in the suprachiasmatic nuclei (SCN) of the hypothalamus, which in turn orchestrates subsidiary oscillators in peripheral organs. The impact of peripheral circadian oscillators upon key metabolic functions has been demonstrated in rodent models, [1]. Moreover, there is growing evidence of a tight reciprocal connection between dysregulation of circadian clockwork and metabolic diseases, including obesity and type 2 diabetes [2–4].

In humans, insulin secretion and glucose homeostasis are orchestrated by the circadian system [2, 5]. Cell-autonomous

clocks have been characterised in human pancreatic islet cells from human individuals [6] and these clocks play a critical role in maintaining proper temporal pattern of the islet hormone secretion in physiology [7]. Moreover, genetic association analyses suggest connections between the circadian clock and the metabolic syndrome, with *NPAS2* and *PER2* polymorphisms being associated with increased blood glucose levels [8] and a *MTNR1B* receptor polymorphism being linked to increased risk for type 2 diabetes [9].

Although molecular clock studies in humans are limited by availability of human tissues, the universal cellular conservation of circadian clock mechanisms makes them tractable for study in human primary cells [6, 10]. Cellular oscillators studied in primary skin fibroblasts in vitro represent an excellent experimental system allowing insights into circadian function in vivo in humans [11–13]. Using this non-invasive approach, we aimed to unravel whether potential alterations in molecular properties of the circadian oscillator are associated with type 2 diabetes glycaemic control in humans. To provide such mechanistic insights, comparative transcriptomic and chromatin immunoprecipitation (ChIP) analyses were conducted in skin fibroblasts derived from non-diabetic control individuals and diabetic individuals with different degrees of glycaemic control.

Methods

Participant characteristics and study design Eleven non-diabetic volunteers, eight non-obese volunteers with type 2 diabetes and nine obese volunteers with type 2 diabetes were enrolled in this study. All participants gave informed consent and the study had ethics committee approval (CER11-015). Participants were included according to the criteria listed in electronic supplementary materials (ESM) Table 1, based on a detailed questionnaire completed during the pre-selection process. The study was registered at [ClinicalTrials.gov](https://www.clinicaltrials.gov) (registration no. NCT02384148). The participant age, sex and chronotype were comparable between the non-diabetic control and type 2 diabetes groups, and differences between the groups stemmed from HbA_{1c} and BMI values (Table 1 and ESM Table 1). A detailed list of medications taken by each participant is presented in ESM Table 2. All study participants filled out the Munich Chronotype Questionnaire (MCTQ; [14]), allowing calculation of MSF_{sc} values that characterise an individual's chronotype. To minimise bias in metabolic variables stemming from acute alimentary variations, participants were subjected to isoenergetic diets calculated as 146.44 kJ (35 kcal) per kg ideal body weight $\pm 10\%$ per day, 15% proteins, 35% lipids and 55% carbohydrate, administered during the 24 h prior to blood sampling and skin biopsy, followed by overnight fasting starting from 22:00 hours.

Primary dermal fibroblast culture, in vitro synchronisation and real-time bioluminescence recording Cutaneous biopsies were taken from each participant's shoulder between 08:30 and 09:00 hours and processed as described previously [11]. Cells were transduced with *Bmal1* (also known as *Arntl*)-*luciferase* (*luc*) and *Per2-luc* lentivectors, synchronised with a 100 nmol/l dexamethasone pulse and subjected to circadian bioluminescence recording as described in [11], either in the presence of FCS or the individual's own sera in recording medium. Because of the absence of significant changes in cellular circadian characteristics in the presence of different concentrations of human serum in the medium (ESM Fig. 1), and due to material limitations, experiments in presence of an individual's serum contained 15% serum added to the recording medium. Bioluminescence from each dish was continuously monitored for 1 week using a Hamamatsu photomultiplier tube detector assembly. Photon counts were integrated over intervals of 1 min. After removing the first oscillation cycle (to avoid a potential bias stemming from the immediate early response to synchronisation), the remaining cycles were analysed with the Actimetrics LumiCycle programme and detrended by a moving average with a window of 24 h [10].

Harvesting of sera Blood samples (50 ml) were collected between 08:30 and 09:00 hours in clot-activator vacutainers and

13 ml of each sample was sent to the Geneva University Hospital laboratory for insulin, blood glucose, HbA_{1c}, cortisol and lipid measurements (reported in ESM Table 3). The remainder was processed for serum collection by centrifugation, following 30 min incubation at room temperature.

Lentivector production *Bmal1-luc* lentiviral particles [11] were produced by transient transfection in 293T cells using the polyethylenimine method [15]. Lentiviral particles were harvested at 48 h post-transfection, 100-fold concentrated, titred and used for the transduction of fibroblast cells with multiplicity of infection (MOI) of 3.

Quantitative real-time PCR Total RNA was extracted from fibroblasts using RNA spin II kit (Macherey-Nagel, Oensingen, Switzerland). Total RNA (0.5 μ g) was reverse-transcribed using Superscript II reverse transcriptase (Invitrogen, Zug, Switzerland) and random hexamers, and PCR-amplified using the SYBR green master mix (Applied Biosystems, Zug, Switzerland). Mean quantitative real-time PCR (qRT-PCR) values for each sample were calculated from technical duplicates of each and normalised to the mean of two housekeeping genes (*HPRT* [also known as *HPRT1*] and *9S*). The primer sequences are listed in ESM Table 4.

RNA sequencing Fibroblasts were harvested 24 h following synchronisation and total RNA was extracted. RNA sequencing (RNAseq) libraries were generated with the Illumina TruSeq protocol (San Diego, CA, USA) according to the manufacturer's instructions, starting with 300 ng of RNA. Then, 49 bp paired-end reads were generated with an Illumina HiSeq 2000 sequencer, and reads were mapped with GEMtools v1.6.2 ([16]; <http://gemtools.github.io/>) onto the human genome GRCh37. RNAseq library preparation and data analysis are described in detail in ESM Methods.

Chromatin immunoprecipitation assay Synchronised cells were fixed with 1% (wt/vol.) formaldehyde (final concentration) and sonicated to prepare chromatin suspensions. ChIP was carried out using anti-circadian locomotor output cycles kaput (CLOCK) antibody (Covalab, Villeurbanne, France) or control IgG (Abcam, Cambridge, UK). Real-time ChIP-quantitative PCR was performed using the primers described in ESM Table 4. PCR products were subjected to agarose gel electrophoresis. Relative enrichment was calculated as the difference between CLOCK and control antibody signals and normalised to the respective input signals.

Statistical analyses Participant characteristics are presented as mean \pm SD, except for period length (mean \pm SEM). A Mann-Whitney *U* test was applied to compare period length and transcript expression levels between groups. To assess the circadian characteristics of quantitative PCR data, we used a

Table 1 Participant characteristics

Participant ^a	Sex	Age (years)	BMI (kg/m ²)	Chronotype (MSF_sc) ^b	Glycaemia (mmol/l)	HbA _{1c} (mmol/mol)	HbA _{1c} (%)	HOMA-IR ^c	Period length ^d (h)
ND 1 ^e	F	40	19.0	2.9	5.7	33	5.2	NA	24.9
ND 3 ^f	F	47	22.8	4.7	6.2	37	5.5	2.0	25.5
ND 4 ^e	M	46	24.8	4.3	6.0	36	5.4	1.5	23.9
ND 5 ^{e,f}	M	64	24.0	3.0	5.2	34	5.3	NA	23.8
ND 6 ^f	M	56	24.5	2.6	5.3	31	5.0	NA	24.2
ND 7	F	62	19.6	3.4	5.8	40	5.8	1.7	23.8
ND 8	F	52	24.6	2.3	5.8	37	5.5	1.5	25.7
ND 9 ^{e,f}	F	57	20.7	4.8	4.8	36	5.4	NA	24.6
ND 10 ^f	M	49	23.5	NA	5.8	34	5.3	1.7	25.2
ND 11	F	46	23.3	4.2	5.7	30	4.9	1.4	24.5
ND 13 ^e	F	51	21.7	3.8	5.5	30	4.9	1.3	25.5
All ND		52 ± 7	22.6 ± 2.0	3.5 ± 0.8	5.6 ± 0.4	34.4 ± 3.2	5.3 ± 0.3		24.7 ± 0.22
DNOwc 3	F	44	28.9	4.8	8.7	54	7.1	1.7	23.9
DNOpc 4	M	70	28.7	3.7	9.8	61	7.7	4.7	24.2
DNOpc 5	M	68	27.4	3.9	9.3	58	7.5	23.9	23.7
DNOwc 6 ^{e,f}	M	69	23.0	2.0	6.5	39	5.7	1.8	25.3
DNOpc 8	M	58	27.4	3.4	8.5	83	9.7	1.7	23.5
DNOpc 9 ^e	M	79	27.0	2.1	6.3	64	8.0	1.2	23.2
DNOwc 10 ^e	M	65	24.2	4.3	5.8	40	5.8	NA	25.5
DNOwc 13 ^e	M	63	28.6	5.2	7.7	54	7.1	21.5	23.8
All DNO ^g		65 ± 10	26.9 ± 2.2	3.7 ± 1.1	7.8 ± 1.5	56.6 ± 13.9	7.3 ± 1.3		24.1 ± 0.29
DOwc 1 ^e	M	49	33.8	4.0	7.1	43	6.1	14.1	25.0
DOwc 2 ^e	M	63	32.7	3.5	7.6	46	6.4	17.9	25.0
DOpc 11 ^f	M	40	33.9	7.0	10.6	73	8.8	NA	23.8
DOpc 12 ^{e,f}	M	72	36.3	2.7	5.5	63	7.9	NA	25.1
DOpc 14 ^e	M	71	35.4	2.1	9.8	81	9.6	1.7	24.0
DOpc 15 ^{e,f}	F	53	34.2	3.6	6.0	95	10.8	8.6	23.8
DOpc 16	F	51	38.9	5.9	8.4	101	11.4	3.3	24.3
DOpc 17 ^f	F	53	45.2	3.2	14.2	62	7.8	NA	23.6
DOwc 18	M	48	49.1	NA	5.9	49	6.6	12.1	24.4
All DO ^g		56 ± 11	37.7 ± 5.7	4.0 ± 1.7	8.3 ± 2.8	68.1 ± 21.0	8.4 ± 1.9	9.6 ± 2.6	24.3 ± 0.19
All DNO+DO ^g		59 ± 11	32.6 ± 7.0	3.8 ± 1.4	8.1 ± 2.2	63.0 ± 18.5	7.9 ± 1.7		24.2 ± 0.17
All wc ^g		58 ± 10	31.5 ± 8.7	4.0 ± 1.1	7.0 ± 1.1	46.4 ± 6.2	6.4 ± 0.6	11.5 ± 3.4	24.7 ± 0.25
All pc ^g		62 ± 12	33.4 ± 5.9	3.7 ± 1.6	8.8 ± 2.6	74.1 ± 15.2	8.9 ± 1.4	6.4 ± 3.1	23.9 ± 0.17

^a Participants with type 2 diabetes were assigned to subgroups: well-controlled (wc) or poorly controlled (pc), based on HbA_{1c} value ≤54.1 mmol/mol (7.1%) and >54.1 mmol/mol, respectively

^b MSF_sc corresponds to the mean sleep phase corrected for sex and cumulative sleep debt calculated from the Munich Chronotype Questionnaire (MCTQ; [14]). MSF_sc value cannot be calculated for participants who need an alarm clock to wake up during free days

^c HOMA-IR could not be calculated when insulinaemia value was missing

^d Period length obtained at the screening with *Bmal1-luc* reporter in the presence of 15% own serum in the recording medium. The indicated numbers represent an average of two parallel dishes (technical duplicate). Significant shorter period length in the fibroblasts established from individual whose type 2 diabetes is poorly controlled (HbA_{1c} >54.1 mmol/mol) compared with their well-controlled counterparts ($p=0.019$)

^e Participant biopsies used to measure *ICAM1* and core-clock transcript expression around the clock (Fig. 3 and ESM Fig. 3)

^f Participant biopsies used to measure CLOCK binding on the *ICAM1* promoter region (Fig. 4)

^g Value for whole group is expressed as mean ± SD, except for period length value, which is expressed as mean ± SEM

DNO, type 2 diabetes non-obese group; DO, type 2 diabetes obese group; F, female; M, male; NA, non-applicable; ND, non-diabetic control group; pc, poorly controlled; wc, well controlled

Cosine fitting method (CosinorJ) [17]. Profiles analysed by CosinorJ were qualified as 24 h rhythmic for $\chi^2 < 0.5$ within the period length range of 18–30 h and as non-rhythmic if $\chi^2 \geq 0.5$ or outside this period length range. The statistical significance of the differences in period length, measured in cells established from skin biopsies derived from non-diabetic and diabetic individuals in presence of either FCS or patient's sera in recording medium, was assessed by Mann–Whitney *U* test. Correlations between individual metabolic variables and fibroblast period length were determined by Spearman's rank correlation coefficient. Multiple correction testing of the *p* value associated with the ρ value was performed using the Benjamini–Hochberg procedure [18]. To represent the relationship between HbA_{1c} and period length, Lowess (locally weighted scatterplot smoothing) regression and a linear model with third-degree polynomials were used [19]. For all analyses, statistical significance was attributed for *p* values <0.05. All analyses were performed using SPSS 20.0 (IBM, New York, NYUSA) and R 3.5.1 (<https://cran.r-project.org/bin/windows/base/old/3.5.1/>, accessed 2 July 2018).

Results

Circadian oscillations in primary skin fibroblasts from non-diabetic and diabetic individuals in the presence of their own serum Consistent with previous reports [11], we found high-amplitude anti-phasic circadian oscillations of *Bmal1-luc* and *Per2-luc* reporters in human primary skin fibroblasts (Fig. 1a). *Bmal1-luc* oscillatory profiles were recorded from fibroblast cells derived from 17 individuals with type 2 diabetes (eight non-obese and nine obese) and compared with 11 non-diabetic counterparts (Table 1). Recording for each cell line was first conducted in the presence of either 15% FCS or 15% of each individual's own serum (ESM Fig. 1). While no significant differences in period length were observed within the non-diabetic control group when analysed in the presence of FCS or human serum, the oscillation period was significantly shorter in the type 2 diabetes group (particularly the obese subgroup) in the presence of participants' own sera (ESM Table 5). We next compared cellular oscillations in the non-diabetic and type 2 diabetes groups in the presence of each individual's own serum and also performed 'cross-serum' experiments using serum from a person of the other subgroup (non-diabetic control or type 2 diabetes, respectively) (ESM Fig. 2a). In this experiment, no significant effects of serum factors from non-diabetic and diabetic individuals on fibroblast rhythm were observed (ESM Fig. 2b).

Therefore, for the rest of the study we conducted the analyses of cellular circadian properties in the presence of 15% of each participant's own serum, representing the closest approximation to the *in vivo* situation. Under these conditions, no significant differences in oscillation period length were

observed between the fibroblasts derived from skin biopsies from non-diabetic individuals and individuals with type 2 diabetes (Fig. 1b, Table 1). Consistently, comparison of temporal expression profiles of endogenous core-clock components in the fibroblasts derived from non-diabetic and diabetic individuals' skin biopsies also revealed no significant differences in expression levels of *BMAL1*, *REV-ERB α* (also known as *NR1D1*), *DBP* and *PER1* transcripts (ESM Fig. 3).

HbA_{1c} inversely correlates with skin fibroblast circadian period in individuals with type 2 diabetes To test the possible association of cellular circadian characteristics with the progression of type 2 diabetes pathophysiology, we calculated the correlations between clinical and metabolic characteristics of the participants and *Bmal1-luc* period length measured in skin fibroblasts *in vitro* (Table 2). Strikingly, our analysis revealed a significant inverse correlation between HbA_{1c} blood levels and circadian period length measured in skin fibroblasts *in vitro*, considering study participants overall (Table 2). When the correlation analysis was performed separately for each study group, this inverse correlation was maintained within the type 2 diabetes group: cells from individuals with type 2 diabetes with highest HbA_{1c} exhibited the shortest oscillation period (Fig. 2, Table 1). Moreover, fibroblasts derived from individuals with poorly controlled type 2 diabetes (HbA_{1c} >54.1 mmol/mol [7.1%]) had a significantly shorter period length than those from individuals with controlled type 2 diabetes (HbA_{1c} ≤54.1 mmol/mol [7.1%]) (23.9 ± 0.17 h vs 24.7 ± 0.25 h respectively, Table 1). This inverse correlation was not observed for the non-diabetic control group (Fig. 2).

The correlation between HbA_{1c} values and cellular period length recorded *in vitro* was stronger for the subgroup of individuals who were non-obese and had type 2 diabetes (ESM Fig. 4a), consistent with the significant inverse correlation between blood glucose and cellular oscillation period in type 2 diabetes (ESM Fig. 4b). In addition, in the diabetic non-obese group, there was a significant inverse correlation between serum triacylglycerol levels and skin fibroblast period length (ESM Fig. 4c, ESM Table 3). No significant correlation was observed between BMI and cellular period length (Table 2). Finally, age and sex did not have an impact on the cellular oscillatory properties (ESM Figs 5, 6).

RNAseq analysis of human skin fibroblasts from the type 2 diabetes group reveals genes differentially expressed in concordance with diabetes severity and individual chronotype To obtain mechanistic insights into the inverse correlation between circadian period of the skin fibroblasts and HbA_{1c} values that we observed in individuals with type 2 diabetes, we performed global gene expression profiling. RNAseq analysis was conducted in cells derived from individuals with type 2 diabetes 24 h following *in vitro* synchronisation. Type 2 diabetes samples were grouped according to cellular period length (Table 3) and

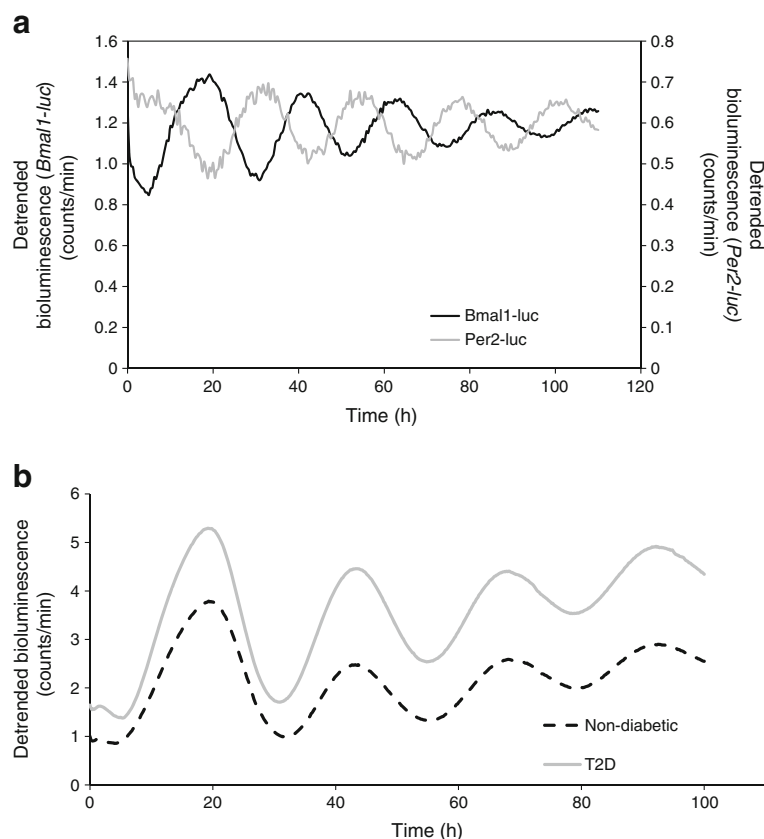


Fig. 1 Circadian oscillation measurements in primary human fibroblasts established from skin biopsies. **(a)** Normalised bioluminescence data for *Bmal1-luc* and *Per2-luc* oscillation profiles recorded in the presence of 15% FCS, from a representative skin fibroblast cell line established from non-diabetic control individuals, synchronised with a single dexamethasone pulse and transferred to the Actimetrics LumiCycle for bioluminescence recording. Raw bioluminescence data were filtered by a moving

average transformation (detrended), as described in the Methods. **(b)** Comparison of average circadian oscillation profiles (detrended) of *Bmal1-luc* bioluminescence recorded from primary human fibroblasts established from non-diabetic participants ($n=11$) and participants with type 2 diabetes (T2D) ($n=17$) in the presence of each participant's own serum. No significant difference was observed in oscillator characteristics between non-diabetic and diabetic groups

Table 2 Correlations between the period length of *Bmal1-luc* reporter recorded in skin fibroblasts synchronised in vitro and clinical and metabolic characteristics of individuals

Variable	ρ	p value	Adjusted p value
BMI (kg/m^2)	-0.326	0.09	0.18
Blood glucose (mmol/l)	-0.444	0.018	0.06
HbA _{1c} (mmol/mol)	-0.515	0.005	0.042*
Diabetes duration (years)	-0.396	0.037	0.092
Insulin (pmol/l)	-0.171	0.395	0.564
Cortisol (nmol/l)	-0.041	0.836	0.916
Total cholesterol (mmol/l)	0.021	0.916	0.916
LDL-cholesterol (mmol/l)	0.09	0.647	0.809
HDL-cholesterol (mmol/l)	0.278	0.153	0.255
Triacylglycerols (mmol/l)	-0.488	0.008	0.042*

Correlations between clinical and metabolic characteristics of all the study participants and fibroblast period length (h) ($n=28$) were determined by Spearman's rank correlation coefficient (ρ). Multiple correction testing of the p value associated with Spearman's rank correlation was performed using the Benjamini–Hochberg procedure [18]. * $p<0.05$

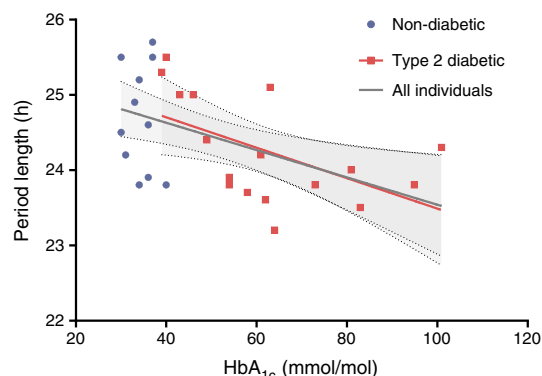


Fig. 2 Inverse correlation between fibroblast circadian period length and HbA_{1c} in individuals with type 2 diabetes. Correlations are presented between HbA_{1c} values measured on the test day and the oscillation period length (*Bmal1-luc*) recorded from human primary skin fibroblasts in the presence of 15% of each individual's own serum. Spearman correlation factor (ρ): -0.515 for all participants ($n=28$), adjusted p value = 0.042 (Table 2); -0.592 for obese and non-obese individuals with type 2 diabetes grouped together ($n=17$), $p=0.012$; -0.030 for non-diabetic volunteers ($n=11$), $p=0.930$. The dotted lines surrounding the lines of best fit indicate the 95% CI

differential gene expression analysis was performed by permutation analysis, randomly sampling 100 technical replicates per comparison in order to robustly call differentially expressed genes (ESM Methods). Interestingly, such analysis conducted between cells derived from the participants with type 2 diabetes with either early or late chronotype (as evaluated by MSF_sc) revealed 1048 differentially expressed genes (Table 3). Next, analysis considering cells from type 2 diabetes samples based on an individual's clinical characteristics revealed several groups of differentially expressed genes involved in cell surface receptor signalling, cell adhesion and additional pathways (ESM Table 6).

Importantly, RNAseq analysis of genes differentially expressed between cells exhibiting a 'short' period length (defined by us as ≤ 24 h) and those with a 'long' period length (≥ 25 h) identified *ICAM1*, encoding for a cell adhesion molecule (Table 3). Moreover, *ICAM1* was differentially expressed depending on BMI (ESM Table 6).

***ICAM1* exhibits different temporal patterns in human skin fibroblasts derived from non-diabetic individuals, individuals with well-controlled type 2 diabetes and individuals with poorly controlled type 2 diabetes** *ICAM1* gene expression profiling from cells harvested 'around the clock' (i.e. at different times of day after circadian rhythm synchronisation) revealed higher expression levels in the fibroblasts derived from individuals with poorly controlled type 2 diabetes (exhibiting $\text{HbA}_{1c} > 54.1$ mmol/mol /7.1%), as compared with the cells established from counterparts with well-controlled blood glucose levels (Fig. 3a). This difference was observed at all time points, and it reached statistical significance at circadian time (CT) 20, with CT defining the time after in vitro synchronisation (Fig. 3a). In view of previously reported evidence implicating *ICAM1* in type 2 diabetes pathology [20], we compared its temporal expression between the fibroblasts derived from skin biopsies from non-diabetic control individuals and individuals with type 2 diabetes (Fig. 3b). *ICAM1* exhibited very low expression levels in fibroblasts derived from control individuals, and this expression was not qualified as circadian rhythmic according to CosinorJ analysis [17]. Of note, our previously published circadian transcriptome from human skeletal muscle biopsies derived from non-diabetic individuals revealed robust circadian expression of *ICAM1* in vivo [21]. *ICAM1* levels increased two- to 3.5-fold in the counterparts established from

individuals with type 2 diabetes between CT 24 and CT 32. Overall, *ICAM1* expression in cells established from skin biopsies from individuals with type 2 diabetes synchronised in vitro exhibited a circadian profile, with a period length of 26.44 ± 0.32 h according to the CosinorJ algorithm, and the highest expression occurring at CT 24 (Fig. 3b).

The circadian transcription factor CLOCK binds rhythmically to the *ICAM1* gene in fibroblasts from individuals with type 2 diabetes and correlates with gene expression

CLOCK has been suggested to induce *ICAM1* transcription through its binding to the *ICAM1* gene E-box-like enhancer region in cultured mouse hepatocytes [22]. To test whether a similar mechanism may account for differential rhythmic expression of *ICAM1* in human fibroblasts, we performed a ChIP assay. This assay demonstrated CLOCK binding to the *ICAM1* promoter region in human fibroblasts (Fig. 4a). Temporal analysis of CLOCK binding to *ICAM1* promoter in synchronised skin fibroblasts revealed a lower level of binding in fibroblasts derived from non-diabetic control individual biopsies compared with the cells established from diabetic counterparts. This difference was particularly pronounced at CT 20 (Fig. 4b), where the binding of CLOCK reached its maximum in cells derived from individuals with type 2 diabetes, prior to the maximum *ICAM1* mRNA expression measured at CT 24 by qRT-PCR (Fig. 3b), suggesting a potential role of CLOCK binding in the upregulation of *ICAM1* rhythmic expression in individuals with type 2 diabetes.

Discussion

Our study provides for the first time compelling evidence for a significant inverse correlation between HbA_{1c} , as well as blood glucose measured on the trial day, and the circadian period length of the cellular oscillators within skin fibroblasts derived from individuals with type 2 diabetes (Fig. 2 and ESM Fig. 4b). No such correlation was observed between HbA_{1c} values and period length in non-diabetic control individuals, likely due to their tightly controlled glucose homeostasis resulting in a narrow range of HbA_{1c} values. Indeed, the HbA_{1c} range was 30–40 mmol/mol (4.9–5.8%) in control individuals, as compared with 38.8–101 mmol/mol (5.7–11.4%) in individuals with type 2 diabetes. It should be noted that the main medications

Table 3 Genes differentially expressed among individuals with type 2 diabetes based on circadian characteristics criteria in RNAseq dataset

Characteristic	Criteria		Differentially expressed genes ($p < 0.05$)
	Short (≤ 24 h)	Long (≥ 25 h)	
Period length recorded in skin fibroblasts in vitro	Short (≤ 24 h) $n = 9$	Long (≥ 25 h) $n = 5$	<i>ICAM1</i>
Chronotype evaluated by MSF_sc	Low (MSF_sc ≤ 3) $n = 4$	High (MSF_sc ≥ 4) $n = 6$	1048 significant genes

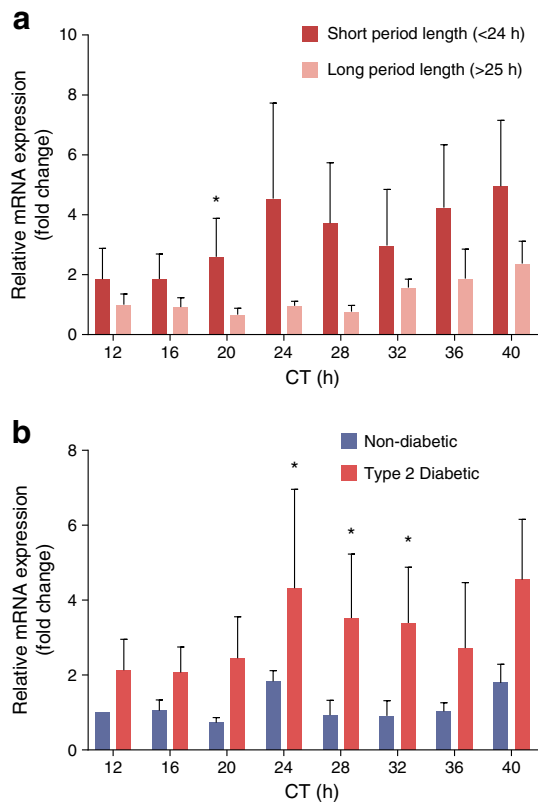


Fig. 3 *ICAMI* temporal expression profiles in individuals with type 2 diabetes and non-diabetic volunteers. *ICAMI* mRNA expression was monitored over the 24 h time period in human primary fibroblasts cultured in the presence of 15% FCS and synchronised with a dexamethasone pulse. qRT-PCR was performed using RNA obtained from fibroblasts established from individuals designated by the superscript ^e in Table 1. *ICAMI* mRNA expression was normalised to the average of *HPRT* and *9S* housekeeping gene expression. The data represent the mean \pm SEM for each time point. CT 12 corresponds to the time point 12 h after the synchronisation pulse. (a) *ICAMI* mRNA expression in primary fibroblasts cultured from eight individuals with type 2 diabetes: four with a short *Bmal1-luc* circadian period length (≤ 24 h) and $HbA_{1c} \geq 54.1$ mmol/mol (7.1%) (participants DNOpc 9, DNOwc 13, DOpc 14 and DOpc 15; see Table 1) and four with a long *Bmal1-luc* period length (≥ 25 h) and $HbA_{1c} < 54.1$ mmol/mol (7.1%) (participants DNOwc 6, DNOwc 10, DOWc 1 and DOWc 2; see Table 1), with equal distribution of obese and non-obese participants in each group ($*p < 0.05$ vs long period length; Mann–Whitney *U* test). (b) *ICAMI* mRNA expression in primary fibroblasts cultured from four non-diabetic control volunteers (participants ND 1, ND 4, ND 5 and ND 13; see Table 1) and nine individuals with type 2 diabetes (designated by the superscript ^e in Table 1) ($*p < 0.05$ vs control individuals; Mann–Whitney *U* test). The average profile for cells derived from skin biopsies from individuals with type 2 diabetes qualified as circadian rhythmic with period length of 26.44 ± 0.32 h by the CosinorJ algorithm [17] ($\chi^2 = 0.39$), whereas the temporal profile of cells established from skin biopsies from non-diabetic individuals did not qualify as significantly circadian

administered chronically to the study participants from the diabetic group were metformin and insulin (ESM Table 2), whereas the non-diabetic individuals did not receive these medications. Thus, we cannot formally exclude a bias in our analyses stemming from chronic medication administration.

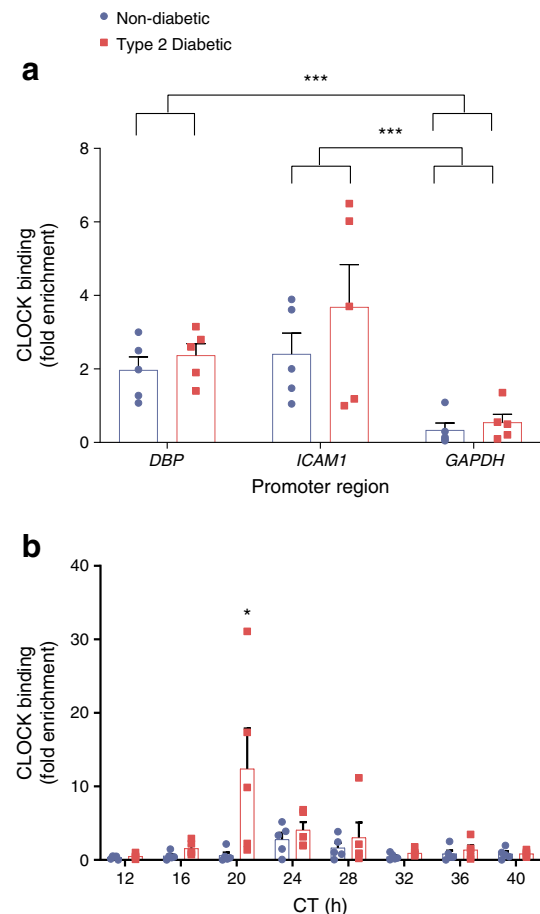


Fig. 4 Binding of CLOCK to the *ICAMI* promoter in human primary skin fibroblasts. ChIP assays were carried out with anti-CLOCK antibody or control IgG. DNAs were amplified with primers (listed in ESM Table 4) specific for human *ICAMI*, *DBP* (positive control) or *GAPDH* (negative control) promoter regions, quantified by qRT-PCR and normalised to control immunoprecipitation with IgG. The data represent the mean \pm SEM for each time point. (a) Binding of CLOCK to the *ICAMI* gene enhancer region in human primary fibroblasts established from five individuals with type 2 diabetes (participants DOWc 6, DNOpc 12, DNOpc 15, DNOpc 11 and DNOpc 17; see Table 1) and five non-diabetic control volunteers (participants ND 3, ND 5, ND 6, ND 9 and ND 10, designated by the superscript ^f in Table 1), 24 h following synchronisation with a pulse of dexamethasone and cultured in the presence of 15% FCS ($***p < 0.001$; Mann–Whitney *U* test). The fold enrichment is normalised to control immunoprecipitation with IgG. (b) Rhythmic binding of CLOCK to the *ICAMI* gene enhancer region over the 24 h time period. Following a dexamethasone in vitro synchronisation pulse, primary fibroblasts established from five individuals with type 2 diabetes (participants DOWc 6, DNOpc 12, DNOpc 15, DNOpc 11 and DNOpc 17; see Table 1) and five non-diabetic control volunteers (participants ND 3, ND 5, ND 6, ND 9 and ND 10, designated by the superscript ^f in Table 1) and cultured in the presence of 15% FCS were harvested and subjected to ChIP assays at the indicated times. CT 12 corresponds to the time point 12 h following the synchronisation pulse ($*p < 0.05$ vs control group; Mann–Whitney *U* test). The fold enrichment is normalised over the level of binding of *GAPDH* negative control region. The average profile of CLOCK binding in fibroblasts established from participants with type 2 diabetes qualified as circadian rhythmic, with a period length of 25.64 ± 0.17 h, by the CosinorJ algorithm [17] ($\chi^2 = 0.48$), whereas the binding of CLOCK in fibroblasts established from non-diabetic participants did not qualify as significantly rhythmic ($\chi^2 = 1.61$)

Furthermore, fibroblast cell transcriptional analysis by RNAseq revealed a significant association between increased expression of the clock-driven *ICAM1* transcript and type 2 diabetes severity (Table 3). Indeed, fibroblasts derived from individuals whose type 2 diabetes was poorly controlled exhibited higher expression levels of *ICAM1* across the entire span of 24 h and showed a short oscillation period, as compared with the cells established from well-controlled counterparts which had a longer period (Fig. 3a). Moreover, *ICAM1* levels were higher overall in cells established from skin biopsies from individuals with type 2 diabetes compared with those originating from non-diabetic participants (Fig. 3b). Consistent with previous observations made in human endothelial cell lines [23], *ICAM1* expression varied around the clock in synchronised skin fibroblasts for all assessed cell groups (Fig. 3a, b). Whereas the temporal profile of *ICAM1* expression in skin fibroblasts from individuals with type 2 diabetes qualified as circadian rhythmic, this was not the case for the cells derived from non-diabetic counterparts, possibly due to the low absolute expression of the gene (Fig. 3b). Of note, temporal expression of *ICAM1* in human skeletal muscle biopsies from non-diabetic participants in vivo is highly rhythmic [21]. The discrepancy in circadian amplitude between the two temporal patterns might be attributed to the difference between in vivo and in vitro conditions, with the absence of continuous entrainment in the latter [21].

Previous studies suggested that CLOCK modulates inflammatory responses via the regulation of proinflammatory molecules such as intercellular adhesion molecule 1 [24]. We now demonstrate CLOCK binding to *ICAM1* promoter and show that this binding was stronger in cells established from skin biopsies from individuals with type 2 diabetes. The peak level of binding narrowly preceded that of *ICAM* transcript expression (Figs 4b, 3b, respectively), suggesting a role for CLOCK binding in the upregulation of *ICAM1* rhythmic expression in type 2 diabetes. One plausible explanation might be that the chronic high glucose level in type 2 diabetes engenders epigenetic changes in the *ICAM1* promoter, rendering it more readily accessible for CLOCK binding. Taken together, our data suggest differential circadian expression of *ICAM1* in skin fibroblasts derived from individuals with poorly controlled and well-controlled type 2 diabetes, perhaps directly driven by CLOCK binding. This raises the possibility of using *ICAM1* as a potential marker predictive of the severity of type 2 diabetes pathology.

The molecular mechanism of the intriguing phenomenon of inverse correlation between type 2 diabetes severity measured by HbA_{1c} and skin fibroblast circadian period cannot be readily explained by our study. One possible scenario might be that chronic exposure to high levels of glucose in type 2

diabetes promotes tissue-specific alterations leading to changed properties of the circadian oscillator. For example, recent studies have demonstrated that modification of proteins by monosaccharides of O-linked β -*N*-acetylglucosamine (O-GlcNAc) might influence phase and period of circadian oscillations [25], suggesting that protein O-GlcNAcylation could directly modify the regulation of clock-controlled genes such as *ICAM1*. It would be of great interest to find out whether core-clock protein glycosylation levels are altered in type 2 diabetes and whether this post-translational modification might contribute to impairment of binding of CLOCK at the *ICAM1* promoter.

Of note, RNAseq analysis of skin fibroblasts derived from individuals with type 2 diabetes revealed 1048 genes differentially expressed according to the chronotype of the individual (MSF_sc, Table 3). Among them, *CYP19A1*, *PAPPA*, *ITIH5*, *GDF15* and *EPAS1* were previously reported to be associated with obesity and type 2 diabetes [24, 26]. It would be of interest to explore the possibility of the individual chronotype alterations associated with severity of type 2 diabetes, along with a potential predisposition for metabolic disease based on individual chronotype.

Reporter-based methodologies such as the one employed here permit much greater flexibility and resolution in the study of intrinsic circadian properties [6, 10–12, 17] compared with in vivo biopsy sampling around the clock [27, 28].

The connections between human type 2 diabetes and circadian function that we uncovered in this work open several paths, which will likely allow exploration of the relationship between molecular clockwork and type 2 diabetes aetiology. Future studies focused upon circadian function in peripheral metabolic tissues such as skeletal muscle and white adipose tissue, both in vivo and in vitro, will doubtless provide additional evidence of this connection, as well as possibly clinically relevant molecular mechanisms to explain it.

Acknowledgements The authors thank I. Wagner, L. Perrin (the Dibner lab), G. Sinyavsky (Florida University, USA), K. Tsutsumi and K. Tamura (Yamaguchi University, Japan) for assistance with the experiments and thank J. M. De Abreu Nunes (Department of Genetics and Evolution, University of Geneva) for help with statistical analyses.

Data availability RNA sequencing data and clinical phenotypic data have been deposited at the European Genome-phenome Archive (EGA), which is hosted by the European Bioinformatics Institute (EBI) and the Centre for Genomic Regulation (CRG), ega-box-1210, under accession no. EGAS00001003622.

Funding This work was funded by the Novartis Foundation for Medical-Biological Research, Jubiläumsstiftung Swiss Life Foundation, Vontobel Foundation and Olga Mayenfisch Foundation (CD) and by SNSF Sinergia grant CRSII3_160741 (SAB, JP, ETD).

Duality of interest The authors declare that there is no duality of interest associated with this manuscript.

Contribution statement FS, A-MM and CD collected the data and drafted the manuscript. PM, CT and JP recruited and enrolled the volunteers. ZP and AG recruited the volunteers. CH, GR and ETD conducted and analysed RNA sequencing. SAB, CP, JP and CD designed the study. All the authors participated in conception and design of the study and in the drafting and approval of the manuscript. CD is the guarantor of this work and, as such, had full access to all the data in the study and takes responsibility for the integrity of the data and the accuracy of the data analysis.

References

- Partch CL, Green CB, Takahashi JS (2014) Molecular architecture of the mammalian circadian clock. *Trends Cell Biol* 24(2):90–99. <https://doi.org/10.1016/j.tcb.2013.07.002>
- Gachon F, Loizides-Mangold U, Petrenko V, Dibner C (2017) Glucose homeostasis: regulation by peripheral circadian clocks in rodents and humans. *Endocrinology* 158(5):1074–1084. <https://doi.org/10.1210/en.2017-00218>
- Marcheva B, Ramsey KM, Buhr ED et al (2010) Disruption of the clock components CLOCK and BMAL1 leads to hypoinsulinaemia and diabetes. *Nature* 466(7306):627–631. <https://doi.org/10.1038/nature09253>
- Perelis M, Marcheva B, Ramsey KM et al (2015) Pancreatic beta cell enhancers regulate rhythmic transcription of genes controlling insulin secretion. *Science* 350(6261):aac4250. <https://doi.org/10.1126/science.aac4250>
- Dibner C, Schibler U (2015) Circadian timing of metabolism in animal models and humans. *J Intern Med* 277(5):513–527. <https://doi.org/10.1111/joim.12347>
- Pulimeno P, Mannic T, Sage D et al (2013) Autonomous and self-sustained circadian oscillators displayed in human islet cells. *Diabetologia* 56(3):497–507. <https://doi.org/10.1007/s00125-012-2779-7>
- Saini C, Petrenko V, Pulimeno P et al (2016) A functional circadian clock is required for proper insulin secretion by human pancreatic islet cells. *Diabetes Obes Metab* 18(4):355–365. <https://doi.org/10.1111/dom.12616>
- Englund A, Kovanen L, Saarikoski ST et al (2009) NPAS2 and PER2 are linked to risk factors of the metabolic syndrome. *J Circadian Rhythms* 7(0):5. <https://doi.org/10.1186/1740-3391-7-5>
- Lyssenko V, Nagorny CL, Erdos MR et al (2009) Common variant in MTNR1B associated with increased risk of type 2 diabetes and impaired early insulin secretion. *Nat Genet* 41(1):82–88. <https://doi.org/10.1038/ng.288>
- Perrin L, Loizides-Mangold U, Skarupelova S et al (2015) Human skeletal myotubes display a cell-autonomous circadian clock implicated in basal myokine secretion. *Mol Metab* 4(11):834–845. <https://doi.org/10.1016/j.molmet.2015.07.009>
- Brown SA, Fleury-Olela F, Nagoshi E et al (2005) The period length of fibroblast circadian gene expression varies widely among human individuals. *PLoS Biol* 3(10):e338. <https://doi.org/10.1371/journal.pbio.0030338>
- Brown SA, Kunz D, Dumas A et al (2008) Molecular insights into human daily behavior. *Proc Natl Acad Sci U S A* 105(5):1602–1607. <https://doi.org/10.1073/pnas.0707772105>
- Saini C, Brown SA, Dibner C (2015) Human peripheral clocks: applications for studying circadian phenotypes in physiology and pathophysiology. *Front Neurol* 6:95
- Roenneberg T, Wirz-Justice A, Mrosovsky M (2003) Life between clocks: daily temporal patterns of human chronotypes. *J Biol Rhythm* 18(1):80–90. <https://doi.org/10.1177/0748730402239679>
- Toledo JR, Prieto Y, Oramas N, Sanchez O (2009) Polyethylenimine-based transfection method as a simple and effective way to produce recombinant lentiviral vectors. *Appl Biochem Biotechnol* 157(3):538–544. <https://doi.org/10.1007/s12010-008-8381-2>
- Marco-Sola S, Sammeth M, Guigó R, Ribeca P (2012) The GEM mapper: fast, accurate and versatile alignment by filtration. *Nat Methods* 9(12):1185–1188. <https://doi.org/10.1038/nmeth.2221>
- Mannic T, Meyer P, Triponez F et al (2013) Circadian clock characteristics are altered in human thyroid malignant nodules. *J Clin Endocrinol Metab* 98(11):4446–4456. <https://doi.org/10.1210/jc.2013-2568>
- Benjamini Y, Hochberg Y (1995) Controlling the false discovery rate: a practical and powerful approach to multiple testing. *J R Stat Soc Ser B Methodol* 57(1):289–300
- Cleveland WS (1981) LOWESS: a program for smoothing scatterplots by robust locally weighted regression. *Am Stat* 35(1):54. <https://doi.org/10.2307/2683591>
- Derosa G, Maffioli P (2016) A review about biomarkers for the investigation of vascular function and impairment in diabetes mellitus. *Vasc Health Risk Manag* 12:415–419. <https://doi.org/10.2147/VHRM.S64460>
- Perrin L, Loizides-Mangold U, Chanon S et al (2018) Transcriptomic analyses reveal rhythmic and CLOCK-driven pathways in human skeletal muscle. *Elife* 7:e34114. <https://doi.org/10.7554/eLife.34114>
- Gao Y, Meng D, Sun N et al (2014) Clock upregulates intercellular adhesion molecule-1 expression and promotes mononuclear cells adhesion to endothelial cells. *Biochem Biophys Res Commun* 443(2):586–591. <https://doi.org/10.1016/j.bbrc.2013.12.022>
- Wang Q, Bozack SN, Yan Y, Boulton ME, Grant MB, Busik JV (2014) Regulation of retinal inflammation by rhythmic expression of MiR-146a in diabetic retina. *Invest Ophthalmol Vis Sci* 55(6):3986–3994. <https://doi.org/10.1167/iovs.13-13076>
- Ramakrishnan SK, Zhang H, Takahashi S et al (2016) HIF2alpha is an essential molecular brake for postprandial hepatic glucagon response independent of insulin signaling. *Cell Metab* 23(3):505–516. <https://doi.org/10.1016/j.cmet.2016.01.004>
- Kaasik K, Kivimae S, Allen JJ et al (2013) Glucose sensor O-GlcNAcylation coordinates with phosphorylation to regulate circadian clock. *Cell Metab* 17(2):291–302. <https://doi.org/10.1016/j.cmet.2012.12.017>
- Wei K, Piecewicz SM, McGinnis LM et al (2013) A liver Hif-2alpha-Irs2 pathway sensitizes hepatic insulin signaling and is modulated by Vegf inhibition. *Nat Med* 19(10):1331–1337. <https://doi.org/10.1038/nm.3295>
- Gomez-Abellan P, Gomez-Santos C, Madrid JA et al (2010) Circadian expression of adiponectin and its receptors in human adipose tissue. *Endocrinology* 151(1):115–122. <https://doi.org/10.1210/en.2009-0647>
- Otway DT, Mantele S, Bretschneider S et al (2011) Rhythmic diurnal gene expression in human adipose tissue from individuals who are lean, overweight, and type 2 diabetic. *Diabetes* 60(5):1577–1581. <https://doi.org/10.2337/db10-1098>

Publisher's note Springer Nature remains neutral with regard to jurisdictional claims in published maps and institutional affiliations.